

## On the Extensive Air Shower density spectrum

ALEKSANDER ZAWADZKI <sup>(1)</sup>, TADEUSZ WIBIG <sup>(2)</sup>, and JERZY GAWIN <sup>(3)</sup>

<sup>(1)</sup> *Collège de France, Paris*

<sup>(2)</sup> *Experimental Physics Dept., University of Łódź, Pomorska 149/153, 90-236 Łódź, Poland*

<sup>(3)</sup> *Soltan Institute of Nuclear Studies, Uniwersytecka 5, 90-950 Łódź, Poland*

(ricevuto ?; approvato ?)

**Summary.** — In search for new methods of determining the primary energy spectrum of Cosmic Rays, the attention was paid to the density spectrum measurement. New methods available at present warrant an accurateness of conclusions derived from the density spectrum measurements. The general statement about the change of the spectral index of the charged particle density spectrum is confirmed very clearly. Results concerning the shower size and primary energy spectra are also presented and discussed. Interesting future prospects for applications of the density spectrum method are proposed.

PACS 96.40.Pq – Extensive air showers..

### 1. – Introduction

The small array of Geiger-Müller (G-M) counters triggered by some coincidence of them gives a very well defined information about the charged particle density at a certain point in the Extensive Air Shower (EAS) plane. The binary type information (nothing registered - at least one particle traversed the detector sensitive area) lead to the limitations of the physical information but, on the other hand, the measurement is free from additional uncertainties introduced always by the amplitude sensitive counters. What is also important the small grammage of G-M counters assure that the charged particles from EAS are what is really measured. This is specially important for a proper taking into account the trigger effects and all the biases close to the small density edge of the measurement domain.

Forty years ago the density spectrum measurements were in the focus of interest of Cosmic Ray (CR) physics. The power-law shape of the spectrum and the behaviour of its spectral index were widely discussed (see e.g. Ref. [1]). The exact measurement with high statistics and a careful statistical analysis was performed and the results were given in Ref. [2] by A. Zawadzki. There was shown clearly the steepening of the density spectrum in the relatively wide range of densities around  $\sim 10 \text{ m}^{-2}$ .

In the present paper we would like to re-examine the same experimental data with the help of much more powerful methods available now. Some assumptions necessary to obtain results in an analytical way are confirmed by numerical calculations.

In the second part of this work we would like to proceed a bit further. The general purpose is to use the old data set to get a new information about the shower size spectrum or even primary particle energy spectrum.

The original work (Ref. [2]) was limited to the charged particle density spectrum problem only. It was obtained as a pure experimental result without any assumptions concerning the EAS picture. The step we want to follow at present is of much more delicate nature because anyway it is relied on the charged particle spatial distribution in the shower plane or even on the knowledge of the primary particle mass and the high energy interaction model, respectively for the size spectrum and for the primary particle energy spectrum case. The only possible way of solving the problem is to use the Monte-Carlo shower simulation calculations believing in their correctness (to some extent, as it will be discussed). For the present work the well-known code CORSIKA v4.12 Ref. [3] has been used.

Finally we want to emphasize that the newly obtained density spectrum confirms the calculations first published forty years ago.

Some short discussion of interesting feature seen for very small particle densities will be given at the end and some future possibilities of using the density spectrum method will be briefly announced.

## 2. – Data

The data were collected in 1954–56 years using the three G–M counter stations each of 18 tubes of 3 cm  $\varnothing$  and 0.013 m<sup>2</sup> sensitive surface. The stations were placed in vertices of a rectangular triangle with catheti of about 8 m. Two of them were used only for triggering (at least one of G–M counters registered something) and the number of G–M signals from the third station was used for further analysis. The question of the efficiency and stability of the whole apparatus was widely discussed in Ref. [2] where it was shown its extremely exact behaviour during all the time the measurement has been performed. The number of registrations (showers registered) was 227712. For the comparison: three previous experiments were made with 3039 (Ref. [4]), 8177 (Ref. [5]) and 22450 (Ref. [6]) statistics and the one of most accurate measurement made at Moscow State University (Ref. [7]) more than twenty years later consists of 11500 events (but for higher density range).

The data are presented in the Fig. 1. For the small values of  $m$  (number of the G–M counters which registered a particle passing through) the statistical accuracy is extremely high. Even for the large showers (big  $m$  values) errors are of order of percents. The 5<sup>th</sup> order polynomial fit in the  $\log N_m$  ( $N_m$  is the number of events with a particular value of  $m$  G–M tubes fired) describe the data (for  $1 \leq m \leq 17$ ) very well (with  $\chi^2/\text{NDF}$  of order of 1). As it was mentioned in Ref. [2] to study the dependence of  $N_m$  with respect to  $m$  the uncertainty at a particular value of  $m$  does not correspond to the statistical measurement error of the point at  $m$  alone. In that sense all the points are not uncorrelated. The proper treatment of the accuracy was discussed in Ref. [2] and will be briefly presented later on.

Due to the problems connected with the interpretation of these data the more convenient presentation is given in the Fig. 2. The ratio of the consequent  $m$ -hit rates is sensitive only to the mean value of the first (and higher orders of course) derivative of

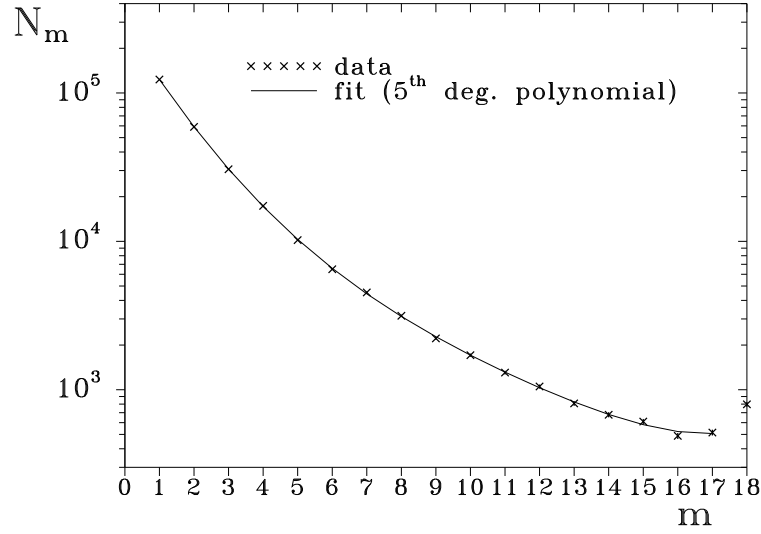


Fig. 1. – Number of events  $N_m$  registered in the experiment with a given value of  $m$  G-M tubes fired. The line is the 5<sup>th</sup> order polynomial fit to the data in the  $(\log N_m - m)$  scale.)

the charged particle density spectrum in a relatively small density range, while the  $m$ -hit rate ( $N_m$ ) depends on the shape of the spectrum as a whole. This point will be discussed below. The line in the Fig. 2 represents the polynomial fit from the Fig. 1. The errors given separately for each point are statistical only. The dashed area is the  $1\sigma$  significance level of the fit so it represents the true error of the measurement.

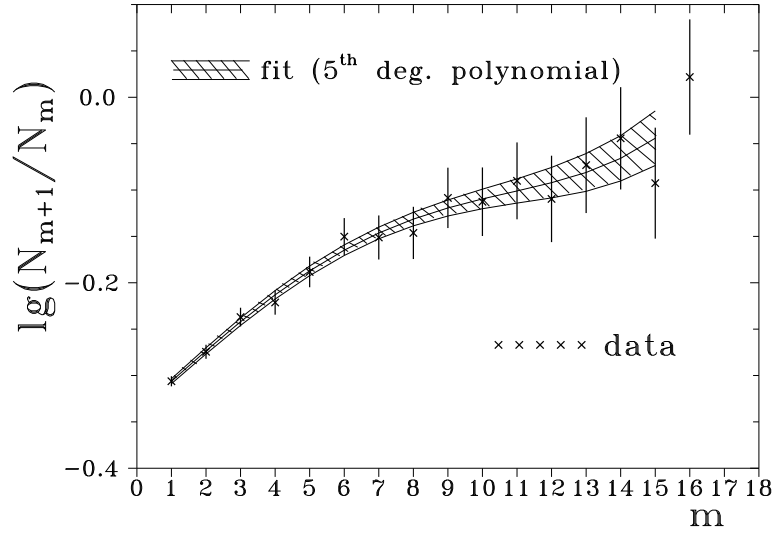


Fig. 2. – The ratio of  $N_{m+1}/N_m$  as a function of  $m$ . The line shows the results of the fit in the Fig. 1. The dashed area represents the  $1\sigma$  significance fit error.

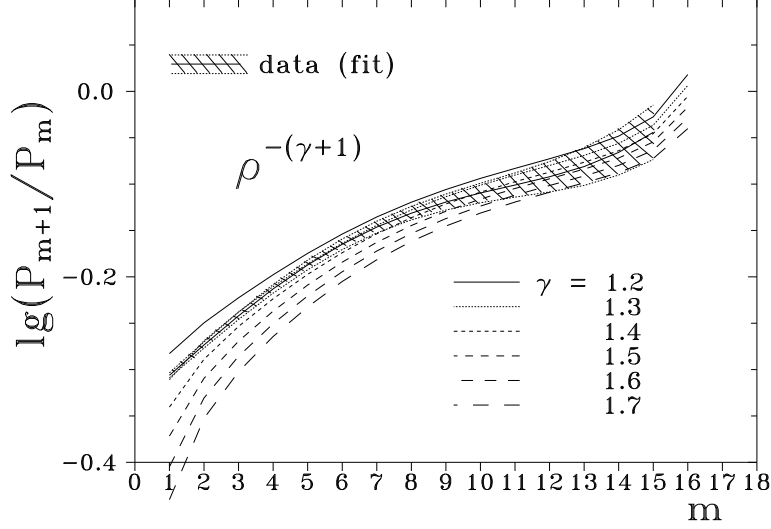


Fig. 3. – The ratio of  $P_{m+1}/P_m$  as a function of  $m$  calculated using Eq. (3) for different constant values of  $\gamma$ . The line shows the experimental result as it was given in the Fig. 1.

### 3. – The analysis

**3.1. The density spectrum.** – As it was briefly discussed the G–M hodoscopic measurement gives the statistically clear basis to evaluate the true charged particle density spectrum. Because the trigger detectors were rather close (in the comparison with the characteristic dimension of the EAS particle lateral distribution) it is quite reasonable to assume that in every case the EAS particle densities in all three G–M stations were exactly the same. On the other hand the spacing between stations was big enough to assume that the particular numbers of particles passing each array fluctuate independently. These two assumptions allow us to calculate the probability that a given particle density leads to the registration of the event:

$$(1) \quad q(\rho)d\rho = d\rho (1 - e^{-sM\rho})^2 f(\rho) \quad ,$$

where:  $s = 0.013\text{m}^2$  is a single G–M tube area,  $M = 18$  is a number of G–M tubes in each station and  $f(\rho)$  is the density spectrum - the point of our interest.

If we denote by  $p(m, \rho)$  the probability that for a given particle density  $m$  of G–M counters register at least one particle then:

$$(2) \quad P_m = \int_0^\infty d\rho q(\rho) p(m, \rho) \quad .$$

The lack of any correlation between EAS particles is assumed. This possibility is a common one but not very obvious (it will be discussed later). Then  $p(m, \rho)$  is given as a binomial distribution (with  $m = 0$  excluded due to the triggering condition).

The first approximation of the density spectrum: the power-law function is used. The aim of the work is to test if the index of this spectrum -  $\gamma$  is constant and to determine

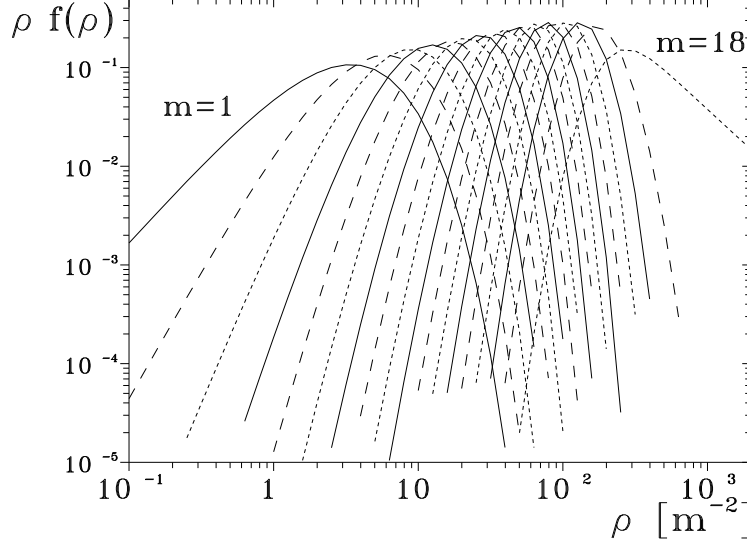


Fig. 4. – The distribution of particle densities giving a contribution to the m-hit rate.

its eventual change as the particle density changes. So we finally get normalized to the unity m-hit counting rate:

$$(3) \quad P_m = \int_0^\infty d\rho (1 - e^{-sM\rho})^2 \binom{m}{M} (1 - e^{-s\rho})^m e^{-s(M-m)\rho} C \rho^{-(\gamma(\rho)+1)},$$

where  $C$  is a spectrum normalization constant.

The Eq. (3) can be evaluated analytically (for constant  $\gamma$ ) for each integer value of  $m$  as it was performed in Ref. [2] in a rather sophisticated manner. The numerical integration confirms the exactness of forty years old calculations. Results show clearly that it is not possible to describe the data with the one constant value of spectrum index. The presentation of  $P_m$  for different  $\gamma$ 's however contains a normalization constant which can be *a priori* different for each value of  $\gamma$  tested. To avoid the confusion in the Fig. 3 the values of  $P_{m+1}/P_m$  are presented.

For such ratios the problem of normalization does not exist (at least if one assumes the change in  $\gamma$  to be not a very dramatic one as is confirmed by the calculations). Detailed analysis of this figure allows us to describe the change of the density spectrum index as a function of  $m$  - the number of G-M tubes with at least one charged particle seen in the event. To obtain the change of the  $\gamma$  with the particle density ( $\gamma(\rho)$  as it is in Eq. (3)) the dependence of the mean density contributing to a particular  $m$  can be calculated as:

$$(4) \quad f_m(\rho) = q(\rho) p(m, \rho) \sim p(m, \rho) \rho^{-(\gamma(\rho)+1)} (1 - e^{-sM\rho})^2.$$

The results are given in the Fig. 4

As it was expected the range of densities contributing to particular  $f_m$  (except the case  $m = 18$ ) is rather narrow so we can use the mean value of each  $f_m(\rho)$  as an average density respected somehow to the value of  $m$ .

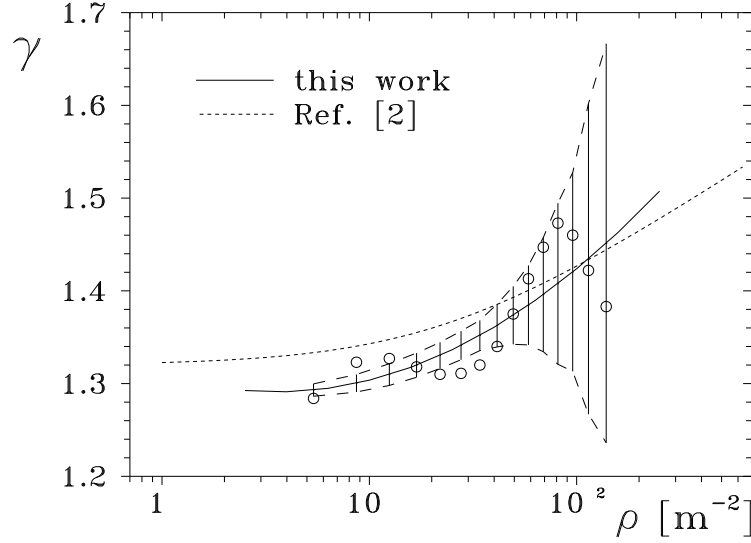


Fig. 5. – The density spectrum index  $\gamma$  as a function of particle density (the dashed area represents a  $1\sigma$  significance region). The dashed line is taken directly from the original work of A. Zawadzki (Ref. [2]).

Finally the  $\gamma(\rho)$  dependence is obtained. It is given in the Fig. 5. For the comparison the original curve of Ref. [2] is also given. The dashed area in Fig. 5 is defined as containing the *true* dependence within 68% probability if its *true* form is a second order polynomial in  $\log \rho$ . (Small circles presented in the Figure represent a measured values approximated by the smooth curve (as it is shown in the Fig. 2) so the systematics seen is rather a result of the method of the presentation than a real effect.) The question of the statistical significance of the change of the slope is further discussed in Appendix C.

**3.2. The shower size spectrum.** – To obtain the shower size spectrum (its index, assuming that the spectrum is in general of the power-law form) from our data some additional assumptions have to be made. Shower of size  $N_e$  consists of number of particles distributed over some area thus something like a continuous spectrum of particle densities appears with respect to the distance to the shower axis for each EAS. So the Eq. (1) has to be modified to:

$$(5) \quad q(\rho) = \int d\vec{r}_0 \int \int d\theta d\varphi g(N_e, \theta, \varphi) \left(1 - e^{-sM\rho(r)}\right)^2,$$

where:  $\vec{r}_0$  is a shower axis position,  $\theta$  and  $\varphi$  are the shower zenithal and azimuthal angles (the azimuthal angle dependence is important here because the G-M counters have a tubular effective volume and are separated by some distance one from another in the array of each station). The particle density  $\rho(r)$  at the detector site is obviously a function of the distance from the detector to the shower axis measured in the shower plane –  $r$  (as it is given explicit in the Eq. (5)), but also of  $N_e$  and both inclination angles. Of course the density distribution of the particular shower due to the physics of the shower development is not an unique function of parameters listed above. Its shape

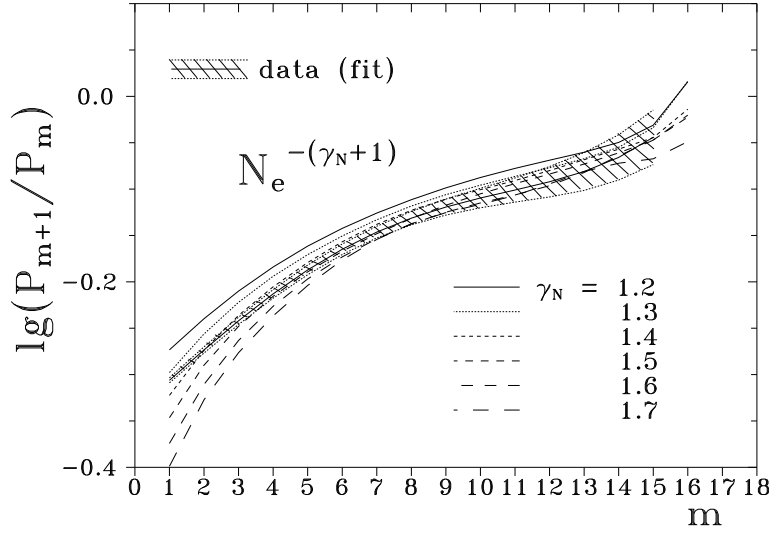


Fig. 6. – The ratio of  $P_{m+1}/P_m$  as a function of  $m$  calculated using Eqs.(3) and (5) for different constant values of size spectrum index  $\gamma_N$ .

fluctuates about the "mean distribution". Regarding those fluctuations and making other simplifying assumptions some connections between the density and size spectra can be found, but the results of such investigations can be misleading (see e.g. Ref. [8]).

In the present paper we would like to present results of the full integration of Eq. (5) and then of Eq. (3). To proceed with Eq. (5) some knowledge of the EAS charged particle distribution and its fluctuations is needed. For this purpose we have used the CORSIKA v 4.12 shower simulation program. The lateral distribution of electrons from the simulated events has been parameterized in a form of:

$$(6) \quad r^2 \rho_e(r) \sim N_e \left( \frac{r}{R_0} \right)^\alpha \left( 1 + \frac{r}{R_0} \right)^\beta$$

for each individual shower. Then the fluctuations from shower to shower and correlations between the distribution parameters were described analytically (to some reasonable extension). Then the Monte-Carlo shower generator was created which for a given set of  $(N_e, \theta, \varphi, \vec{r}_0)$  values returns three mean densities of charged particles at each of three G-M stations positioned exactly as they were forty years ago in Łódź. The integrals in the Eq. (5) were performed by Monte-Carlo and finally the results presented in the Fig. 6 have been obtained for different constant values of size spectrum index  $\gamma_N$ .

The line shows the experimental result as it was given in the Fig. 2.

The result is at the first look rather surprising. In comparison with the density spectrum index the size index variation seen is statistically negligible ( $1\sigma$  effect). Further examinations will be done after the results concerning primary energy spectrum will be given.

**3.3. The energy spectrum.** – The next step is the analysis of the primary particle energy spectrum. This needs another probabilistic function to be assumed. The energy

spectrum is to be used in a convolution with the previously discussed size spectrum and the probability density describing the possibility of producing the shower of the size  $N_e$  (within  $dN_e$ ) by the primary particle of energy equal to  $E$ . Even such a complex evaluation is greatly simplified in a comparison with the reality. The primary CR consist of not only one kind of particles. It can be assumed that there are protons and all the heavier nuclei up to about iron in a comparable and *a priori* unknown proportions (when grouped into five groups: p,  $\alpha$ 's, C–N–O, Ne–Si and  $\sim$ Fe). The development of a shower depends on the nature of the primary particle, so the densities of shower particles at the observation level differ in EAS initiated by the CR particles of the same energy but of different mass.

The second point we have to face to is that obviously the same shower size can be produced by the primary particle of different primary energies (even if its mass is the same). One shower can develop deeper in the atmosphere (due to probabilistic nature of the process) thus the primary particle energy needed to give size of  $N_e$  can be smaller than the energy of the shower which starts at a very top of the atmosphere. According to this it can be expected that the particle density lateral distribution should be no longer treated as a function of the shower size (and angles) only ,as it was done before in the Eq. (5).

The general formula for a density spectrum evaluation from the primary CR energy spectrum can be written as:

$$(7) \quad q(\rho) = \sum_A \int dE h_A(E) \int d\vec{r}_0 \int \int d\theta \, d\varphi \, g_{AE}(N_e, \theta, \varphi) \left(1 - e^{-sM\rho(r)}\right)^2, \quad ,$$

where:  $h_A(E)$  is an energy spectrum of a particular CR particle type and density  $\rho$  is not only a probabilistic function of  $N_e, \theta, \varphi$  and the distance from the shower core (like it was in the Eq. (7)) but also of the set  $(A, E)$  values what is a result of the shower development fluctuations described above.

Of course information about primary mass composition is anyway included in the all-particle energy spectrum. However the summation over  $A$  in the Eq. (7) can be at the moment neglected assuming overall energy spectrum  $h(E)$ . The remaining dependencies on  $A$  value (in  $g(N_e)$ , and  $\rho(r)$  functions) will be neglected also and the functions used further on should be treated as averaged over  $A$ .

With the help of the CORSIKA simulation program the parameters of the shower charged particle lateral distribution  $\rho$  ( $\alpha, \beta$  and  $R_0$ ) were parameterized not only with respect to the  $N_e$  but also the rather consistent description has been found of the value  $N_e / \langle N_e \rangle$  where  $\langle N_e \rangle$  is the mean value of the shower size for EAS induced by the primary particle of energy  $E$ . The fluctuations of  $N_e$  with respect to the mean value were also considered.

With all these assumptions the integration of the Eq. (7) was performed by Monte-Carlo method. Then using the Eq. (3) the results presented in the Fig. 7 were obtained for different values of the index  $\gamma_E$  of the primary CR energy spectrum  $h(E) \sim E^{-(\gamma_E+1)}$ .

The line shows the experimental result as it was given in the Fig. 2.

The results are very similar to the one obtained for the size spectrum evaluation. The change of the power-law index, substantial for the density spectrum, is not seen for the energy spectrum as well.



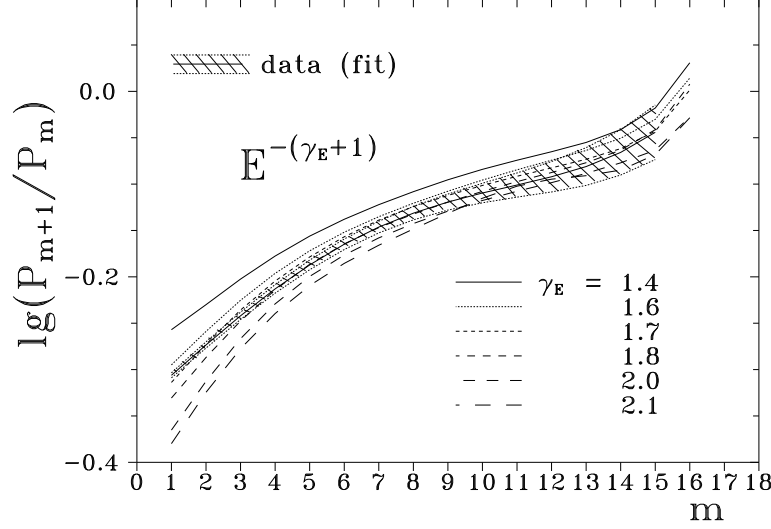


Fig. 7. – The ratio of  $P_{m+1}/P_m$  as a function of  $m$  calculated using Eqs.(3) and (7) for different constant values of energy spectrum index  $\gamma_E$ .

#### 4. – Discussion

**4.1. Size and energy spectra.** – First we want to show quantitatively the reason of the disappearing of the change of the power-law indexes  $\gamma_N$  and  $\gamma_E$  while the index change for the density spectrum,  $\gamma$ , is unquestionable.

The Figures 8 (a) and (b) are analogous to the Fig. 4. They present the distributions of shower sizes (a) and primary energies (b) contributing to the registration of a particular number of  $m$  G-M tubes registered charged particles in the event.

In contrast to the Fig. 4 where the distributions were rather well separated, the distributions in the Fig. 8. are very much wider and overlapping. In the Fig.4 the width (FWHM) of the density distribution in the case of  $m = 7$  is comparable with the distance

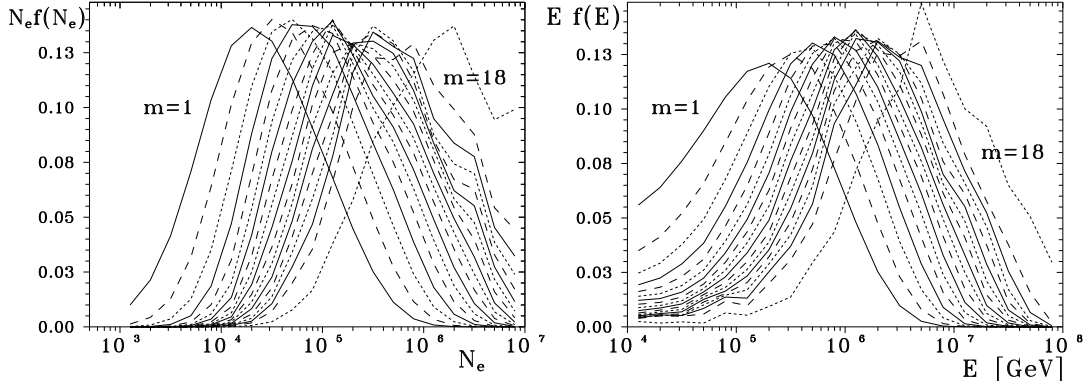


Fig. 8. – The distribution of the shower sizes  $N_e$  (a) and primary energies  $E$  (b) giving a contribution to the  $m$ -hit rate.

between the mean values of  $\rho$  for  $m = 7$  and  $m = 10$  while in the Fig. 8a the FWHM for  $m = 7$  is of order of the distance between  $m = 2$  and  $m = 16$ . For the energies (Fig. 8b) the situation is even worse. This according to the integration procedure leads to smearing out all details in the generally very fast falling spectra.

Due to the large widths of the distributions in the Fig. 8 it is not reasonable to calculate the mean values of  $N_e$  and  $E$  responsible for the spectrum slope at given  $m$ -hit rate as it has been done in the Fig. 5 for the density spectrum. However it is interesting to note that the whole range of sizes and energies for  $m \geq 3$  is of about one decade. It is clear that any change in the spectrum slopes which could be seen by the experiment has to be rather sharp and substantial.

**4.2. Muon density spectrum.** – The interesting possibility is to use the density spectrum method discussed in this paper for a muon component of EAS. Muons are known to be stronger correlated to the primary particle energy and number of muons in the shower fluctuates weaker than the electron shower size (what is due to the difference in their origin mechanism and the shower development geometry). With the help of large EAS array which can be subdivided into smaller parts each giving separately a kind of hodoscopic information about the muon component in the shower the statistic needed can be accumulated relatively fast.

The experiment KASCADE (Ref. [9]) gives an excellent opportunity for such studies. Its muon array part consists of 192 detector stations each of them equipped with four plastic scintillators of area of  $0.81 \text{ m}^2$  placed below the lead and iron shield which stands as a soft shower component absorber. The minimum muon energy required is equal to 300 MeV. Scintillators in every station are viewed by four photomultipliers in such a way that each PM sees two scintillators and the data acquisition system collects hodoscopic information about status of every PM tube. Thus there is a huge amount of “binary” information about every event not disturbed by fluctuations common to “analogous”, pulse-height measurements. This information can be used to obtain a very precise and accurate results concerning the muon density spectrum. The data analysis is in progress and results will be published soon.

The studies of muons in EAS are very important from the point of view of primary mass composition determination. Difficulties concerning estimation of total muon content in individual showers (due to low densities of particles) make the muon density spectrum measurements rather attractive.

## 5. – Conclusions and Summary

The forty years old data were reexamined using more powerful computational methods available at present. The confirmation of the original work (Ref. [2]) results is given. Further evaluation of the same data set shows the general agreement with the power-law spectra of EAS sizes and primary particle energies.

For the extremely small showers there is seen a substantial change of the assumed size and energy spectra shape. However, there are (at least) two undistinguishable possibilities of explanations of that experimental fact. The one is the truncation of the fluctuation distribution of the particle number seen by the limited area detector. This needs to be studied carefully from the point of view of the earth surface EAS experiments intended to fill the gap between the balloon-borne direct measurements and existing ground level experimental results concerning the nature of the primary cosmic ray spectrum. The other interesting aspect of the problem is the exactness of the comparison of small EAS

measurements by the arrays of different geometries (and thus triggers) and positioned at different altitudes.

The standard investigation of such small showers is difficult due to very small particle number, so large areas of relatively sensitive detectors with negligible background noise are needed. The method of the density spectrum measurement by the small hodoscopic counters could be a solution here. To go to smaller energies the new measurement has to be performed with the geometry chosen carefully to get a maximum efficiency in the region of interest.

From the other side, for the density spectrum method the increase of the primary particle energy under study will verify or, at least, confirm in less "Monte-Carlo" dependent way the results about the "knee" problem still discussed by many authors both from experimental and interpretational point of view. The density spectrum method for a muon component of EAS can be used for such purposes.

Concluding we would like to summarize the present work in a few sentences:

- Charged particle density spectrum in the range of  $1 \div 100 \text{ m}^{-2}$  is power-law with the index changing slowly from 1.3 to 1.5.
- Size and primary particle energy spectra were found to be power-law with the indexes  $\sim 1.5$  and  $1.8$  respectively and no significant change of these indexes is seen (see Appendix A).
- Further examination of the small showers behaviour is needed to explain some features seen by the experiment. The density spectrum method can be useful for such investigations (see Appendix B).
- Measurement of the muon density spectrum can give a new interesting look into the problem of the energy spectrum near the "knee" region ( $\sim 10^{15} \text{ eV}$ ).

## APPENDIX A.

### Density spectrum measurements; historical remark

The situation prior to 1957 was summarized by Greisen in Ref. [10]. All measurements show the slight and constant increase of the index in power-law form of the density spectrum. This, in fact, implies that the density spectrum has not a straight power-law form. The measurement of Zawadzki was the first accurate enough which allows one to perform more detailed analysis of the spectral index behaviour (Ref. [11]). The point was that obtained change of the index was rather sharp. For densities smaller than few tens of particles/ $\text{m}^2$  it seems to be constant and the possibility of significant change was indicated for higher densities. This experimental fact gave an assumption to treat the CR spectrum as having a broken power-law form with one index below a certain point and much steeper above. Implications of such a picture are rather far-going and no matter how the original Zawadzki measurement confirmed these speculations the idea of a "knee" or two-component CR spectrum arise and it is still one of the most important features of the cosmic ray phenomenon nowadays.

The paper with the Zawadzki experiment results was originally published in French and distributed not very widely. Confirmation of this fact can be found e.g. in Ref. [12] where still in 1979 year the old Greisen (Ref. [10]) summary of the world data on density spectrum are given without the Zawadzki result. The problem is, in fact, not in omitting the most significant measurement but in referring to the points which are known to be

not exactly correct due to some simplifications made during the data analysis. In Ref. [2] it was shown that results obtained in Ref. [6] should be corrected. Anyhow rather limited statistics of this experiment situate the proposed corrections inside error bars of the original points. For the same reason the other measurements (Refs. [4, 5]) when reexamined, do not contradict the Zawadzki paper conclusions about a sharp change of density spectrum index.

## APPENDIX B.

### Low density part of the spectrum

We want to discuss briefly in this appendix the clear discrepancy with the constant slope of energy and size spectra seen for first 2 or 3 points in the Figs. 6 and 7.

First it has to be mentioned that this can not be explained by the obvious flattening of the particle lateral distribution with decrease of the shower size (thus the primary energy). Smaller showers become “older”, so the continuous change of their lateral distribution is expected and was confirmed in the simulations (using CORSIKA code). This can be a reason of the difference between the size (energy) and density spectra seen in Figs. 3 and 6. However, the effect of the continuous change of the particle lateral distributions in EAS was taken into account in the respective integrals calculations for  $N_e$  and  $E$  spectra – and the sharp decrease of  $\gamma_N$  and  $\gamma_E$  for  $m = 1, 2$  still exists there.

The one most obvious possibility is that the charged particle lateral distribution obtained via CORSIKA program does not correspond to the reality for a very small shower. This way of explanation can explain of course everything, but unless we have no other reason for claims about the CORSIKA incorrectness we have to be careful in such suppositions.

Another possible explanation is connected with the particular shape of the particle number fluctuations at the certain (small) area in the shower plane for very small showers.

This is closely related to the other relatively old experimental effect reported in Ref. [13]. The Authors presented there data taken at Cornell University by recording the pulse height distribution in a single scintillator of area  $0.86\text{m}^2$  with and without the requirement that a single particle be detected simultaneously in another counter a few meters away. The data clearly show that while for the high particle densities the density spectrum has a well defined power-law behaviour with the index of  $-1.62$  then for smaller densities the slope seems to be also  $-1.62$  only if the additional coincidence is required. With the single detector trigger the slope changes dramatically up to  $-3.19$ .

The careful statistical analysis performed during our density spectrum studies allows us to solve “that longstanding mystery” [14]. In the calculations presented above it was assumed that the number of particles fluctuates in a common poissonian way about the mean value given by the particle density times the detector area factor. Assuming that the density spectrum is exactly the power-law one (with, e.g.,  $\gamma = 1.3$ ) we can consider the particle number spectrum seen by the unique area detector. Its distribution is given by

$$(8) \quad P_n = \int_0^\infty d\rho \rho^{\gamma+1} p_n(\rho) \quad .$$

where  $p_n(\rho)$  describes the spread of number of particles seen with respect to the mean value  $\rho$ .

The results for scarcely different  $p_n(\rho)$  distributions are given in the Fig. 9 (divided by the incoming density spectrum to better see the disturbance produced by the fluctuations).

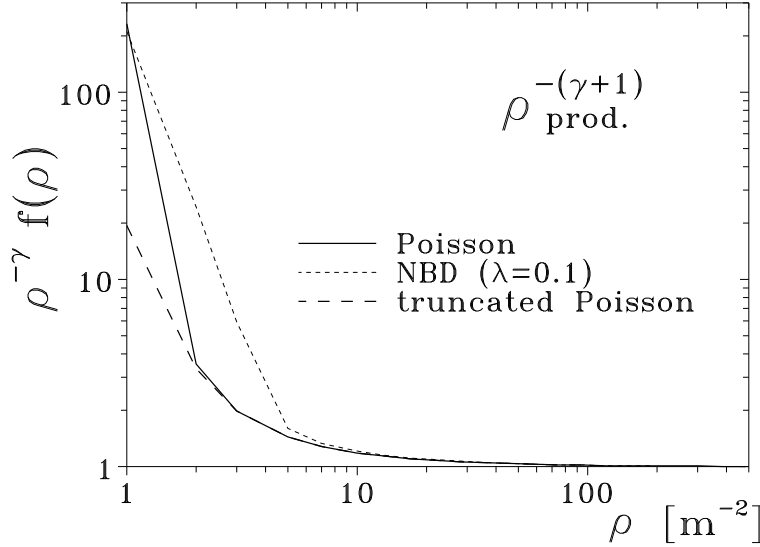


Fig. 9. – The spectrum of the number of particles seen in the detector area divided by the density spectrum of the form  $\rho^{-(\gamma+1)}$  (with  $\gamma = 1.3$ ). The solid line is for pure poissonian fluctuations, the short dashed line is for the Negative Binomial Distribution with the parameter  $\kappa = 0.1$  and the long dashed line represents the truncated Poisson fluctuation.

Curves in the Fig. 9 correspond to the Poissonian distributed fluctuations (solid line)

$$(9) \quad p_n(\rho) = \frac{\rho^n}{n!} e^{-\rho} ,$$

the slightly wider distribution of particle number fluctuations as given by the Negative Binomial Distribution (NBD) (short dashed line)

$$(10) \quad p_n(\rho) = \binom{\rho\kappa + n - 1}{n} \left[ \frac{\kappa}{1 + \kappa} \right]^{\rho\kappa} \left[ \frac{1}{1 + \kappa} \right]^n ,$$

and the Poissonian distribution truncated at  $20\sigma$  (possibility of registration of  $m$  particles when the expected number is  $\bar{\rho}$  is 0 when  $m > \bar{\rho} + 20\sqrt{\bar{\rho}}$ ). The differences are rather small and occur mainly in very tail regions. However, due to the steep density spectrum the tails are extremely important, as it is seen in the Fig. 9. Even the poissonian tails lead to the artificial overabundance of the small particle numbers.

The differences are not so substantial in the Zawadzki experiment like it is presented in the Fig. 9 due to the existence of the three-fold coincidence. This effect was exactly taken into account in our calculations (Eq. (4)). However, it is important to note that even a small change of the fluctuation shape can lead to the change of the expectations for very small showers.

The widening of the fluctuation distribution leads to the more pronounced overestimation of the small particle number rate. The vanishing of the effect with additional coincidence requirement is thus obvious.

Coming back to our main subject, the Zawadzki measurement interpretation, one can see that the rate of events containing small particle numbers looks to be smaller. On the first sight it is hard to imagine that the particle number seen in the detector can

fluctuate narrower than poissonian. However, one has to remember that we have to take into account a very steep density spectrum so the single or two-particle events could occur as a result of large fluctuations for relatively small mean values. The character of the Poisson distribution is such that there is still a possibility of recording an event with any high number of particles for any small expected value. The physical constraints, however, convince one that the unusually high particle numbers simply must not be produced by small showers. Thus, the first approximation poissonian distribution should be truncated at some (distant) point, anyhow. This of course does not disturb the mean values and the spectra for high densities, but can effect the integration in Eqs. (8) and (4) for small values of  $m$  in the way that the calculated above ratio ( $P_m$ ) overestimate the  $m$ -hit ratios for small values of  $m$  as it is shown by the long dashed line in Fig. 9.

### APPENDIX C.

#### Statistical significance of the change of slope of the density spectrum

The analysis of the change of the density spectrum slope presented above has been made using ratios of registered abundances of  $m$  and  $(m+1)$  G-M counters signals. This method assured the continuity of the density (differential) spectrum while changing the slope parameter. In other words we have used the derivative of the spectrum while comparing the experiment with calculations. However when trying to answer the question about the statistical confidence of the measurement the whole experimental information ought to be used (like it is presented in Fig. 1).

The most obvious way of the determination of the correctness of the theoretical description of a measurement is to use the  $\chi^2$  test. With the data given as a simple numbers of counts it is straightforward. Doing the textbook calculations the values of  $\chi^2/NDF$  equal to 1044, 417, 48, 80, 573, 5130, and 18500 have been obtained for the density spectrum indexes  $\gamma$  of 1.2, 1.25, 1.3, 1.35, 1.4, 1.5, and 1.6, respectively. Of course all of them are extremely unacceptable on any confidence level. To understand better the origin of such exceptionally high values a short clarification is needed. It would be at least a misinterpretation to use the numbers given above to determine the statistical significance of the statement on the change of the slope of the density spectrum, specially in connection with the discussion in the preceding Appendix. (One can ask also about the puzzling inconsistency between these values and results given, e.g., in Fig. 3.)

Some useful information can be found investigating contributions to the overall  $\chi^2$  coming from different values of  $m$ . If we define the function  $\chi^2(m)$  as

$$(11) \quad \chi^2(m)/NDF = \frac{\sum_{i=m}^{17} (N_i - N P_i)^2 / N_i}{17 - m},$$

$$\text{where } N = \frac{\sum_{i=m}^{17} N_i}{\sum_{i=m}^{17} P_i} ; \quad (m < 17) ,$$

then respective contributions can be compared. Results of calculations are presented in Fig. 10.

Few important features can be seen. First is that only for the values of index  $\gamma$  in the range  $\sim 1.4 \div 1.5$   $\chi^2/NDF$  of order of 1 can be achieved in some (limited to  $m > 7 \div 9$ ) density range. The second point is the extraordinary rise of  $\chi^2$  for very small values of  $m$ . This is the statistical confirmation of the problem of small density discussed in the Appendix B. The Fig. 10 shows clearly the necessity of the change of the spectrum index from about 1.45 above  $m=7$  to a smaller value (which, however, can not be concluded

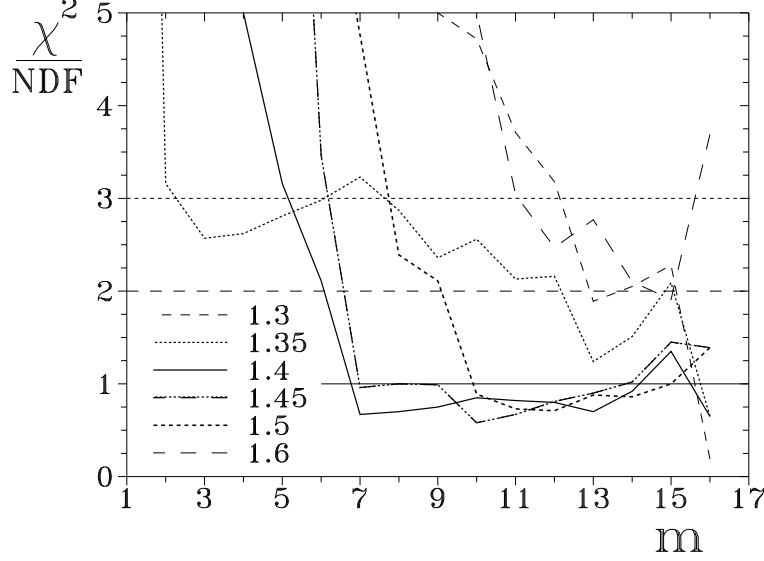


Fig. 10. – Contributions to the overall  $\chi^2$  coming from different parts of the density spectrum ( $m$ ). Lines connect points calculated for integer  $m$  for different values of the density spectrum indexes  $\gamma$ .

form such  $\chi^2$  analysis). Thus the inconsistency of the overall  $\chi^2$  with Fig. 3 seems to be apparent.

The  $\chi^2$  analysis can be of course performed for the shower size and primary energy indexes ( $\gamma_N$  and  $\gamma_E$ ). Respective results are given in Fig. 11 (a) and (b).

Again the overall values of  $\chi^2$  are extremely large, but the plotted different  $m$  contributions confirmed our conclusion made on a basis on Figs. 6 and 7 that the both size and energy spectra are not in contradiction (except of  $m = 1, 2$ ) with the single power-law spectral index of  $\sim 1.5$  and  $\sim 1.8$ , respectively.

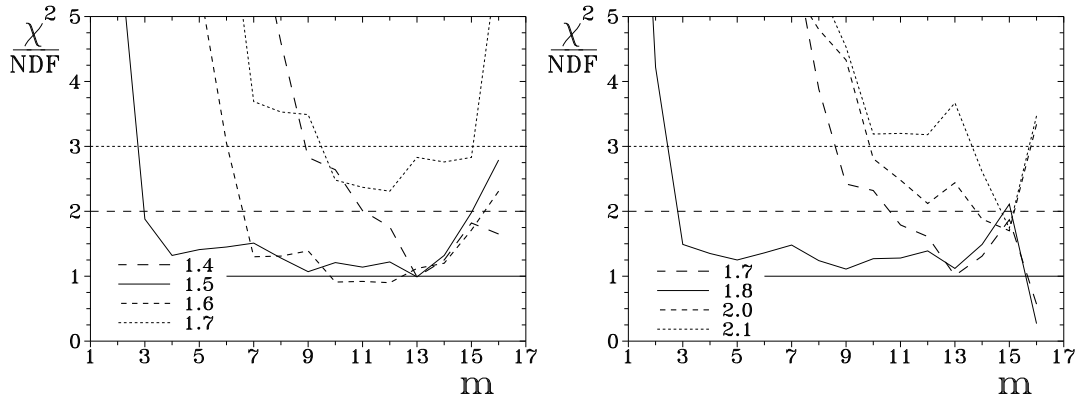


Fig. 11. – Contributions to the overall  $\chi^2$  coming from different  $m$  values for shower size (a) and primary energy (b). Lines connect points calculated for integer  $m$  values for different density spectrum indexes  $\gamma_N$  and  $\gamma_E$ .

## REFERENCES

- [1] W. GALBRAITH, *Extensive Air Showers*, Academic Press Inc., New York (1958).
- [2] A. ZAWADZKI, *Bulletin de l'Académie Polonaise des Sciences*, **5** (1957) 147; *Proc. Intern. Cosmic Ray Conf., Budapest*, (1957) 96; *PhD Thesis* (1958), (unpublished).
- [3] J. N. CAPDEVIELLE *et al.*, *The Karlsruhe Extensive Air Shower Simulation Code CORSIKA*, Kernforschungszentrum Karlsruhe Report No. 4998 (1992); J. KNAPP and D. HECK, *Extensive Air Shower Simulation with CORSIKA: A User's Manual*, Kernforschungszentrum Karlsruhe Report No. 5196B, (1993); J. KNAPP *et al.*, *Proc. XXIV<sup>th</sup> Intern. Cosmic Ray Conf. Rome*, **1** (1995) 403.
- [4] D. BROADBENT, E. KELLERMANN and M. HAKEEM, *Proc. Phys. Soc.*, **63A** (1950) 864.
- [5] A. L. HODSON, *Proc. Phys. Soc.*, **66A** (1953) 49.
- [6] G. COCCONI and V. COCCONI TONGIORGI, *Phys. Rev.*, **75** (1949) 1058.
- [7] G. B. KHRISTIANSEN *et al.*, *Proc. XVI<sup>th</sup> Intern. Cosmic Ray Conf., Kyoto*, **8** (1979) 365.
- [8] N. DOBROTIN *et al.*, *Usp. Fiz. Nauk*, **49** (1953) 185.
- [9] P. DOLL *et al.*, *The Karlsruhe Cosmic Ray Project KASCADE*, Kernforschungszentrum Karlsruhe Report No. 4686, (1990); *Nucl. Phys. B (Proc. Suppl.)*, **14A** (1990) 336; H. O. KLAGES, *Proc. XXIV<sup>th</sup> Intern. Cosmic Ray Conf. Rome*, **1** (1995) 946.
- [10] K. GREISEN, *Prog. Cosmic Ray Physics*, **4** (1956) 1.
- [11] G. COCCONI, *Extensive Air Showers* in *Encyclopedia of Physics* edited by S. FLÜGGE, Springer-Verlag, Berlin-Göttingen-Heidelberg, **XLVI/1**, (1961) 215.
- [12] H. R. ALLAN and S. T. DAVIES, *Proc. XVI<sup>th</sup> Intern. Cosmic Ray Conf., Kyoto*, **8** (1979) 371.
- [13] J. DELVAILLE, F. KENDZIERSKI and K. GREISEN, *Proc. Intern. Cosmic Ray Conf. Moscow*, **2** (1960) 101.
- [14] R. J. O. REID, *Proc. XXI<sup>st</sup> Intern. Cosmic Ray Conf., Adelaide*, **11** (1990) 322.